The published version of the paper "Cerni G., Bassani M. (2017). Naturalistic driving data collection to investigate into the effects of road geometrics on track behaviour. TRANSPORTATION RESEARCH. PART C, EMERGING TECHNOLOGIES, 77, 1-15." is available at: http://dx.doi.org/10.1016/j.trc.2017.01.012

NATURALISTIC DRIVING DATA COLLECTION TO INVESTIGATE INTO THE EFFECTS OF ROAD GEOMETRICS ON TRACK BEHAVIOUR

Cerni G., Bassani M. (*)

Gianluca Cerni

Associate Professor
Department of Civil and Environmental Engineering
Università degli Studi di Perugia
93, via G. Duranti
Perugia, I, 06125
Phone: +39 0755853942
Fax: +39 0755853892
E-mail: gianluca.cerni@unipg.it

Marco Bassani (* = corresponding author)

Associate Professor
Department of Environment, Land and Infrastructures Engineering (DIATI)
Politecnico di Torino
24, corso Duca degli Abruzzi
Torino, I, 10129
Phone: +39 0115645635
Fax: +39 0115645614
E-mail: marco.bassani@polito.it

Submitted to:

Transportation Research Part C: Emerging Technologies (Elsevier)

ABSTRACT

Road designers assume that drivers will follow the road alignment with trajectories centred in the lane, and move at the design speed parallel to the road centreline (i.e., the horizontal alignment). Therefore, they assume that if the horizontal alignment indicates the "designed trajectory", the driving path indicates the "operating trajectory". However, at present, they do not have the necessary tools to measure the relationship between the designed alignment and possible vehicle trajectories.

The paper has two objectives: (a) to develop an understanding of the root causes of differences between road alignment and vehicle trajectories; and (b) to define and calibrate a model that estimates the local curvature of trajectories on the basis of the designed horizontal alignment.

The two objectives were pursued by carrying out a naturalistic survey using vehicles equipped with high precision GPS in real-time kinematics (RTK) mode driven by test drivers on road sections of known geometric characteristics. The results provide an insight into the effects of road geometrics on driver behaviour, thus anticipating possible driving errors or unexpected/undesired behaviours, information which can then be used to correct possible inconsistencies when making decisions at the design stage.

KEYWORDS:

Vehicle trajectory; driving path; road curvature; horizontal alignment; Global Positioning Systems.

1. INTRODUCTION

In every roadway project, the designer assumes that drivers will follow the road alignment with trajectories centred in the lane, and move at the design speed parallel to the road centreline (i.e., the horizontal alignment). The designer selects the most appropriate geometric alignment elements, which consist of tangents and curves (Figure 1a). Where appropriate or indeed compulsory for some standards (AASHTO 2010, Repubblica Italiana 2001a), approaching flatter circular arcs (Figure 1b) or spirals (Figure 1c) are used to obtain a gradual change in alignment curvature between the tangent and more acute circular arcs. The aim is to achieve a harmonious combination of geometric characteristics that will conform to driver expectations and their driving abilities.

According to Messer (1980), geometric features or combinations of adjacent features that surprise the driver lead to unsafe driving conditions. Observations confirm that drivers make fewer errors when the road geometry conforms to their expectations. Since the '80s, road engineers have used the term "design consistency" with respect to methodologies aimed at conforming the alignment of a road to the driver's expectations (Post et al. 1981).

To assess the "design consistency" of a new or existing alignment, Lamm et al. (1999) proposed minimizing operating speed variations and any differences between operating and design speeds, as well as the differences between the operating speeds between successive speed-influencing geometric features. The most practical technique used is represented by the speed profile, in which operating and design speeds are plotted as a function of the alignment chainage. In the last twenty years, the Lamm criteria and/or similar approaches have been used in a number of standards and guidelines (Transportation Research Circular 2011).

Lamm et al. (1995) supported their inferences by noting that the design inconsistencies of a road are associated with a sudden change in its geometric characteristics, which can surprise drivers and lead to significant variations in speed and, sometimes, to driver errors. In their opinion, any divergence between operating and design speed is a consequence of the geometric differences between the actual road alignment and expected driving path.

Accordingly, in the last twenty years designers and researchers have regarded the degree of variation between operating and design speed as a measure of design consistency. Operating speeds can be simply measured in the field with a variety of methodologies and

technologies. Furthermore, literature provides several predictive operating speed models thus avoiding the need to carry out spot speed surveys on roads. In a situation where the design speed is not readily available from original project documents, it can be inferred from road geometric data (Donnell et al. 2009).

However, the use of operating and design speeds appears straightforward when performing a consistency assessment of existing highway sections (Fitzpatrick et al. 2000). Glennon and Harwood (1978) ignored this method when coming up with their conceptual framework for design consistency. This opened the door to alternative methods based on driver's workload (Hancock et al. 1990), and on the assessment of vehicle operations and trajectories.

For example, Messer et al. (1980) used the lateral placement of a vehicle in the lane and drivers' erratic manoeuvres as a means to detect design inconsistencies. Spacek (2005) used measuring posts to detect driving direction as well as transverse distances of the vehicles from the pavement edge. Fitzsimmons et al. (2013) used pneumatic road tubes set-up in a Z-configuration to collect lateral deviation values from a reference line placed at a fixed distance from the horizontal markings. Others have used video recognition techniques at intersections (Messelodi et al. 2005, Mussone et al. 2013) as well as along road sections (Coifman et al. 1998).

Currently, vehicle-tracking surveys for a variety of research purposes are carried out with Global Positioning Systems (GPS) and Inertial (INS) sensors, as well as with hybrid technology combining both sensors (Williams et al. 2012, Tang et al. 2016). These technologies are sufficiently accurate and accessible to provide good quality data on vehicle tracking, in addition to speed and travel time (Patire et al. 2015).

In this context, the paper proposes a new methodology for the comparison of road alignments and vehicle trajectories in order to assess any design inconsistencies of existing roads. To this end, a number of test drivers were involved in field measurement activities along three road sections of two-lane rural highways. Medium class cars equipped with a GPS receiver were employed to collect spatial positioning data.

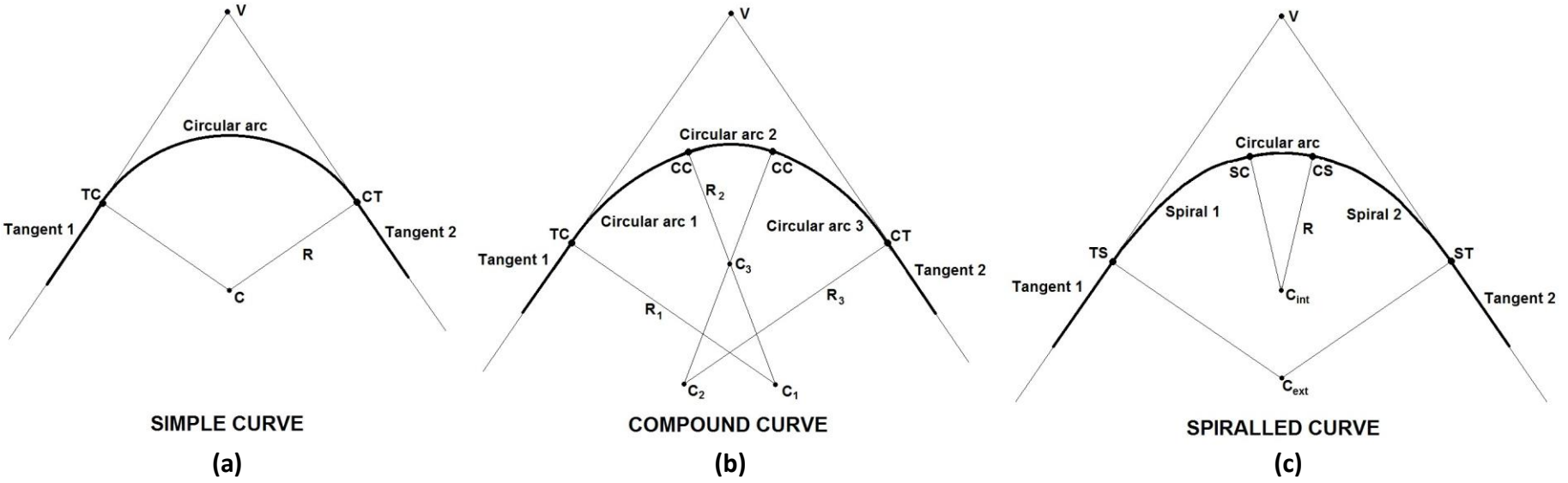

Figure 1. Simple (a), compound (b), and spiralled (c) curves connecting tangents (curve termini are: TC = tangent to curve, CT = curve to tangent, CC = curve to curve, SC = spiral to curve, CS = curve to spiral; curve centres are: C = centre for simple curves, C_1-C_2-C_3 = centres for compound curves, C_{int} = centre of the inner circular arc, C_{ext} = centre of the whole curve)

Curvature diagrams are used here to compare road alignment and vehicle trajectory (i.e., driving path). Curvature trajectories were determined as the inverse of the radius passing through three consecutive surveyed points. Driving path curvatures were first averaged, then compared to the curvature obtained from the as-built horizontal alignment recorded in road cadastre databases (Repubblica Italiana 2001b). In this approach, it is implicitly assumed that if the horizontal alignment indicates the "designed trajectory", the driving path indicates the "operating trajectory". Hence, from their comparison, the geometric consistency of road alignment can be evaluated.

2. VARIABLES AFFECTING VEHICLES TRAJECTORY

Drivers select a road trajectory on the basis of information deriving from the visual observation of roads. The driver converts this road geometric information into pedal and steering wheel movements, with the consequent mechanical conversion of the steering wheel angle into a steering angle of the front axle.

The interaction between the driver and steering wheel depends on how the driver processes the information coming from the road ahead and surrounding area, this being the most important source of information for drivers (Hills 1980). The geometry of road elements like horizontal markings, curbs, traffic barriers, roadside elements (clear zones, barriers, drainage ditches, signage, lateral vegetation, etc.), provide the data which drivers need to elaborate before deciding on a particular driving path.

Several contributions have dealt with the behavioural effects of edge and centreline horizontal markings, both in daytime and night-time driving conditions (Schnell and Zwahlen 1999, Horberry et al. 2006). Experiments conducted at driving simulators confirm that when the visual contrast between edge lines and the pavement is low, drivers tend to decrease their speed (Horberry et al. 2006) and find it difficult to maintain the correct alignment and lateral position of the vehicle in the lane (Horberry et al. 2006, Dijksterhuis et al. 2011). McKnight et al. (1998) noted that the lane keeping performance was compromised only at extremely low levels of contrast between the marking and the pavement. Drivers tend to look ahead at the future path to establish the point at which to start rotating the steering wheel of the vehicle when entering into a curve, assuming the most appropriate steering wheel rotation speed on the basis of the degree of curvature. Land and Lee (1994) observed that the gaze angle correlates with the steering wheel angle, with the visual inspection

preceding the steering wheel action by approximately 1 s. On windy roads, Land and Horwood (1995) demonstrated that most drivers focus their attention on the tangency point within each curve, and use it to determine the driving path curvature. Others observed that optic flow, body orientation and their combination also provide further knowledge useful for controlling the heading angle, which is the angle formed by the direction of motion and the direction of the tangency point (Coutton-Jean et al. 2009).

Prokop (2001) formulated a model to derive vehicle curvature for simple driving tasks, valid for undisturbed driving on roads at moderate speeds and lateral accelerations (Figure 2). In such a scenario, the trajectory curvature depends on the distance of wheelbases from the centre of gravity position, indicated by the front (l_F) and rear (l_R) distances, and on the front steering angle δ (assumed as the average of the two front steering angles) variable as a function of time (t):

$$c(t) = \frac{1}{R(t)} = \frac{\tan\delta(t)}{\sqrt{(l_R + l_F)^2 + l_R^2 \cdot \tan^2 \delta(t)}} \qquad (1)$$

Eq.1 is valid for normal driving conditions, which encompass most of the situations experienced by drivers. It is not valid at high speeds, when a vehicle is subject to severe lateral acceleration that produces over or under-steering effects and involves the yaw dynamic of the vehicle (Prokop 2001). In eq. 1, the steering angle at the front wheels can be substituted by the steering wheel angle at time t, $\delta_s(t)$ in rad/s, assuming the steering wheel to front wheel angle ratio (typically between 12:1 to 20:1 for passenger cars).

Steering parallel to the axis of the road is a difficult task for drivers, because of the continuous change in optical information, which has to be processed (Friedinger 1980). This can cause driver uncertainty and lead to steering corrections. From field observation and as noted by Spacek (2005), it is possible to identify seven types of vehicle trajectory (ideal, normal, correcting, cutting, swinging, drifting, and other, which includes any trajectories that do not come under the definition of the first six) . Observations confirm that different drivers adopt different driving paths on the same curve.

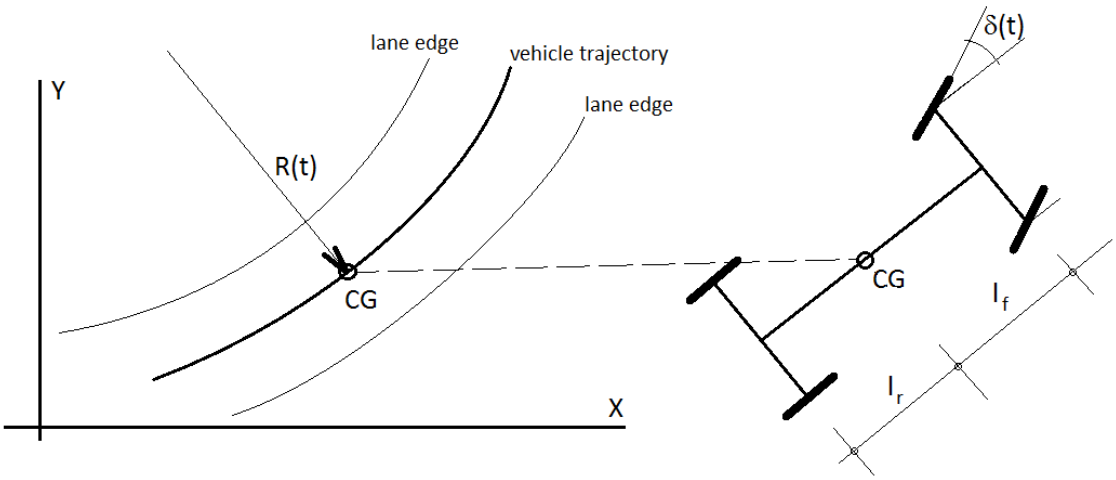

Figure 2. Vehicle trajectory along a lane

When negotiating a simple curve (Figure 1a), the driver rotates the steering wheel anticipating the initial point of curvature along the travelled path (Godthelp 1986). After that, he/she adopts a constant rate of steering wheel angle until he/she reaches the constant value. Stewart (1977) observed that the time used to rotate the steering wheel is approximately double that of the anticipatory time, which represents the interval between the point at which the driver starts the rotation of the steering wheel and the point of curvature (TC or TS in Figure 1).

The existence of a steering time of sufficient length confirms the presence of a spiral trajectory that is always assumed even when transition curves have not been included in the horizontal alignment. Therefore, when the driver anticipates the curve, he/she differentiates the local radius path from the designed curve radius. Consequently, the driver shifts the vehicle laterally in the lane following a flatten trajectory. This type of manoeuvre allows a gradual variation in speed when necessary, and limits any discomfort to drivers and occupants produced by the lateral acceleration. However, when vehicles shift laterally, they may interact dangerously with other vehicles. To limit lateral shifts, designers can select an appropriate combination of road alignment elements and, if required, use spiral transitions.

3. NATURALISTIC DRIVING DATA COLLECTION AND TREATMENT

At present, road engineers do not use models to estimate the effect of the projected road alignment on potential vehicle trajectories. If a knowledge of the effects of road geometrics

on driver behaviour were available and possible driving errors or unexpected/undesired behaviours foreseen, then due consideration could be given to the reversal or modification of any inconsistent design decisions.

With this in mind, the authors pursued two objectives in this paper: (a) an understanding of what can cause vehicle trajectories to diverge from the road alignment; and (b) the definition and calibration of a general model able to provide the local curvature of trajectories on the basis of the design curvature. These two objectives were pursued by conducting a naturalistic survey on instrumented vehicles driven by test drivers on road sections of known geometric characteristics. The following paragraphs introduce the details of this observational investigation.

3.1 Case studies

Three different sections of two-lane rural highways were investigated. The first section was 13.8 km in length (road designation SP170/2+SP169), the second 13.3 km (road designation SP415/1), and the third 6.5 km (road designation SP444/1), for a total length of investigated road of 33.6 km. As per the modelling methodology that will be presented later in the paper, the curvature diagram of the three sections and the two directions (indicated with the letter A and B) are shown together in Figure 3. In the diagram, a positive curvature characterizes right-hand curves, while a negative curvature indicates left-hand curves. Furthermore, the three sections and two directions are illustrated using artificial tangent sections of 1 or 2 km in length.

Figure 3 also highlights the differences and similarities between the three sections; in particular, it is evident that section #3 is characterized by a curve of shorter radii than sections #1 and #2. Table 1 lists the geometric characteristics collected from the as-built cadastral database for tangents, curves, and grades, the combination of which determines a high variation of speeds and steering angles along the same path.

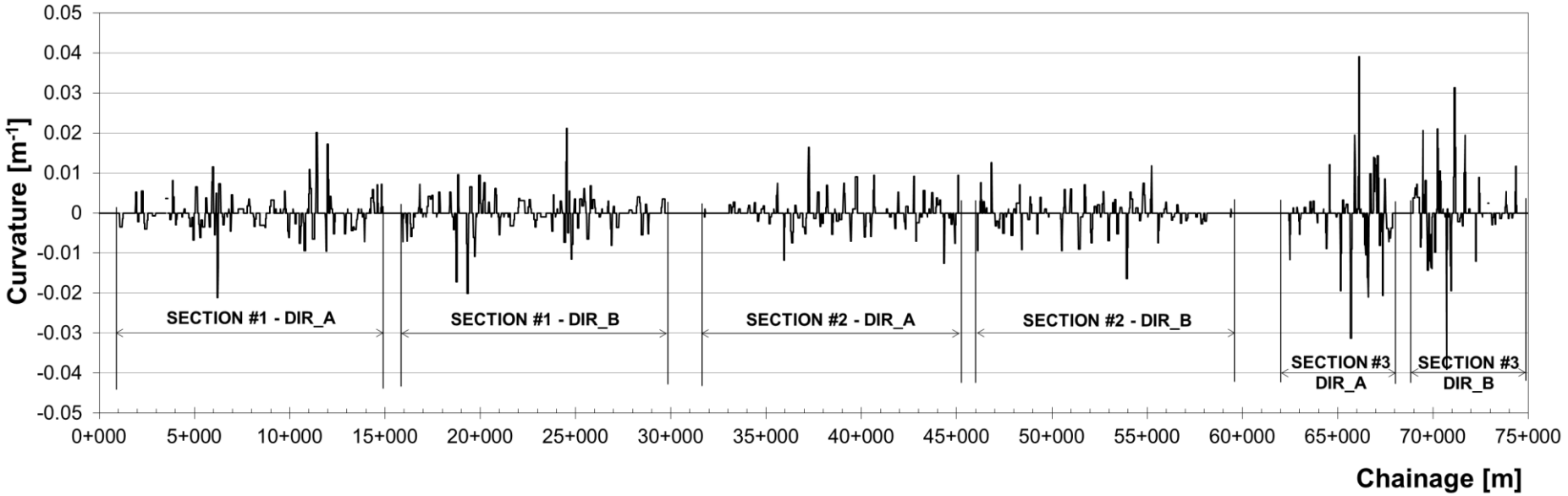

Figure 3. Plan view and curvature diagram of the three road segments analysed as case studies

Table 1. Statistics for tangent, curves and grades derived from the as-built cadastral database, and number of drivers involved

Geometric characteristics		Section #1	Section #2	Section #3	Sections 1-3
Road designation		SP170/2+SP169	SP415/1	SP444/1	-
Length [km]		13.8	13.3	6.5	33.6
Minimum tangent length [m]		17.6	52.3	31.8	17.6
Maximum tangent length [m]		645.6	1260.9	1020.9	1260.9
Minimum radius [m]		47.4	61.0	25.59	25.59
Maximum radius [m]		1369.9	1000	1000	1369.9
Maximum grade (%)		8.3	4.6	6.2	8.3
Number of tangents with length	<100 m	36	20	18	74
	≥ 100 m, < 200 m	17	16	9	42
	≥ 200 m, < 400 m	5	11	3	19
	≥ 400 m, < 800 m	3	2	0	5
	≥ 800 m	0	1	1	2
Number of curves with radius	<100 m	5	3	11	19
	≥ 100 m, < 200 m	20	18	6	44
	≥ 200 m, < 400 m	16	10	3	29
	≥ 400 m, < 800 m	3	10	5	18
	≥ 800 m	17	11	5	33
Length of grades with slope	< -5%	806.5	0	0	806.5
	≥ -5%, < -3%	1069.7	191.9	0	1261.6
	≥ -3%, < -1%	526.0	758.5	0	1284.5
	≥ -1%, < +1%	3061.2	4353.4	1509.2	8923.9
	≥ +1%, < +3%	3018.0	4580.8	215.3	7814.1
	≥ +3%, < +5%	1133.9	505.9	1450.71	3090.58
	≥ +5%	0	0	942.89	942.89
Number of drivers		7	7	17	31

The as-built horizontal alignment has been obtained from the cadastre road database of the Province of Perugia (Italy), and formed according to the prescriptions of Italian law (Repubblica Italiana, 2001b), which regulates the formation of the road cadastre of Italian Public Administrations. The cadastre database contains a spatial points sequence in the cartographic coordinates WGS84. The identification of road elements was undertaken by the Province of Perugia, assuming simple or compound curves (according to Figure 1a and 1b), since no evidence was found from collected data to support the inclusion of spirals in curves.

3.2 Collection of naturalistic driving spatial data

The naturalistic in-field investigation was carried out with medium size cars of the drivers involved in the naturalistic observation (i.e., Fiat Bravo, Alfa Romeo 156, Peugeot 206, BMW Serie 3, etc.). The driving behaviour adopted by the owners reflected their familiarity with the driven cars. The vehicles were monitored using a double frequency GPS receiver (Table 2), with the antenna mounted on a magnetic pedestal on the car-roof, and the receiver located in the vehicles. A fixed master station enabled a post-differential correction that

resulted in the spatial data points being recorded to a high degree of accuracy (1 ÷ 5 cm) and with a sampling frequency of 1 Hz. This sampling frequency was adjusted following a preliminary pilot field investigation that evidenced some noise affecting the accuracy of the collected spatial data points at higher frequencies

The on-board crew was composed of the driver, an operator dedicated to the acquisition and management of data from the GPS receiver, and a second operator dedicated to the collection of driving information (i.e., presence of constraining vehicles, unexpected driving events) on the basis of a common time scale with the first operator. A total of 21 drivers (17 males and 4 females) aged between 20 and 50 years were involved with some of them driving multiple times to give a total of 31 driving experiences.

Surveys were carried out during off-peak hours to limit the effects of other vehicles on driver trajectory choice. Any environmental factors and traffic conditions which could impact on driver speed and trajectory selection during the period of observation were duly noted. Any data affected by such factors were then excluded from the database during the post-processing phase, in order to gather spatial data of trajectories affected by the road geometrics only.

Spatial data points were used to form a database containing the cartographic coordinates (Est, Nord and Z - geodetic elevation), with reference to the curvilinear abscissa and to the GPS time in the same format shown in Table 3. In the same table, the distances and chainage are those calculated by the GPS device and refer to a specific driving experience.

Table 2. GPS receiver specifications

Type	TOPCON LEGACY-E
Constellation	GPS, GLONASS
Frequencies	L1, L2
Survey modality	Kinematic
Antenna	GPS TOPCON PG-A1
External Antenna	Yes
RTK (real time kinematic)	Yes
Positioning [cm]	1-5
Cut-off angle [°]	15

Table 3. Example of data extracted from the database (acquisition frequency of 1 Hz)

Trajectory #2 (SP415_1)						GPS Time		
Point #	Trajectory coordinates [m] Est	Nord	Z	Distance [m]	Chainage [m]	Seconds in Week	Time	Δt [s]
1	2307893.807	4756457.724	165.804	4.46293	0.00000	375309	00:00:01	1
2	2307897.935	4756459.420	165.834	5.95057	4.46293	375310	00:00:02	1
3	2307903.569	4756461.335	165.844	6.67608	10.41349	375311	00:00:03	1
4	2307909.973	4756463.221	165.887	7.39477	17.08958	375312	00:00:04	1
5	2307917.063	4756465.321	165.954	8.56522	24.48434	375313	00:00:05	1
6	2307925.228	4756467.908	166.011	9.90399	33.04957	375314	00:00:06	1
7	2307934.656	4756470.941	166.063	11.10011	42.95355	375315	00:00:07	1
8	2307945.235	4756474.302	166.093	11.56129	54.05367	375316	00:00:08	1
9	2307956.240	4756477.845	166.072	12.00644	65.61495	375317	00:00:09	1
10	2307967.674	4756481.508	166.045	12.82375	77.62139	375318	00:00:10	1

3.3 Association of as-built alignment and naturalistic driving trajectories

Figure 4 depicts the trajectory data point for each of the 7 drivers involved along a segment of Section #2 in both directions (the as-built horizontal alignment), so a total of 15 different lines are represented. The curvature of each constituent point of a driving path was estimated as the reciprocal of the circle radius passing through three consecutive points. The curvature value was then associated with the central point of each tern.

Each trajectory has a different length, so for the purposes of comparison all data points were associated with the specific chainage of the closest point of the road alignment, following the algorithm described here and supported by the diagram of Figure 4.

The generic point of each trajectory (Q_j) was projected along the perpendicular to the as-built horizontal alignment, to estimate the curvilinear abscissa (i.e., chainage). In the first step, the algorithm estimates the parameters m_i and q_i of the straight lines passing through each pair of points $\overline{P_iP_{i+1}}$, obtained from the discretization of the as-built alignment according to the following equation:

$$y = q_i + m_i \cdot x \tag{2}$$

From every Q_j, the perpendicular line to the polyline P_i was then estimated using the following equation:

$$y = q_i^* - \frac{1}{m_i} \cdot x \tag{3}$$

where q_i^* was estimated by solving the same eq. 3 assuming x and y equal to the coordinates of point Q_j.

With eq. 3, several S_j points of intersection with the extension of each pair of points $\overline{P_iP_{i+1}}$ were identified. The shortest $\overline{Q_jS_j}$ segments were then evaluated and the S_j^* point (the closest S_j to Q_j) was then considered. The chainage of Q_j was finally assumed equal to the S_j^* chainage measured along the as-built polyline.

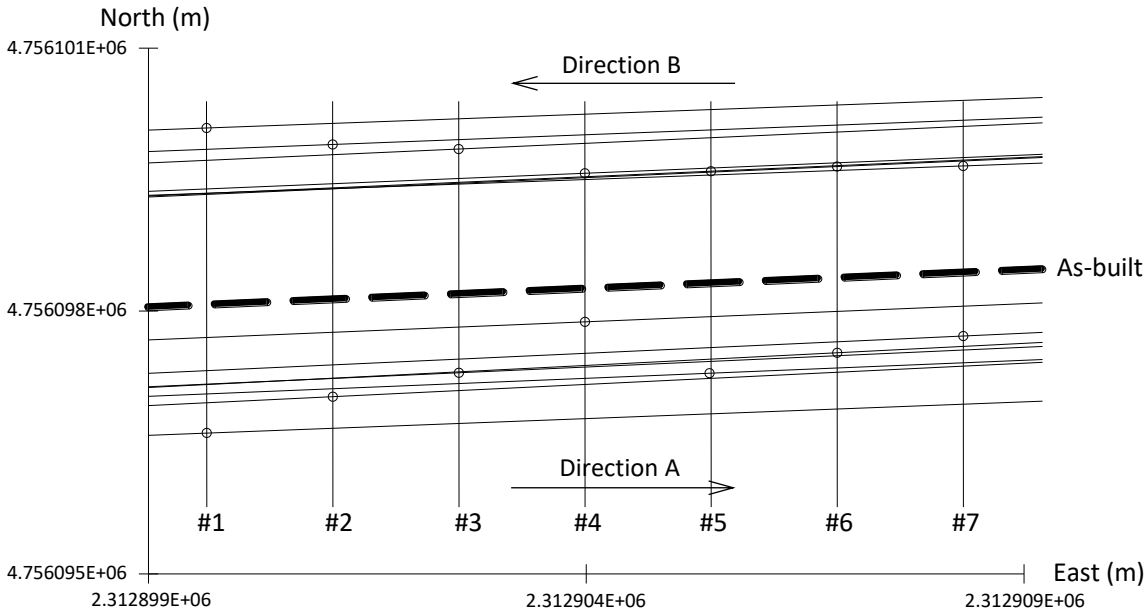

Figure 4. Representation of the trajectories traversed by the 7 drivers (indicated with #) along a segment of Section #2

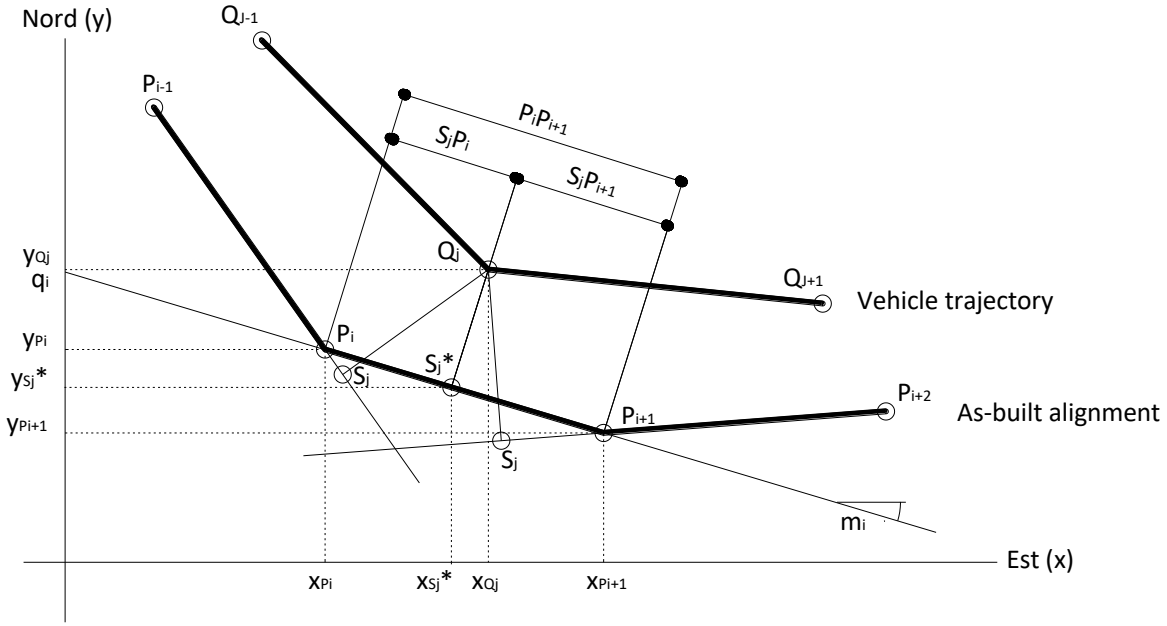

Figure 5. Representation of the geometric parameters considered in the algorithm used to estimate the chainage of point Q_j

The data were filtered to exclude portions of the database where vehicle speed was affected by the presence of other vehicles. The operation was carried out on the basis of the GPS time recorded by the second operator. As a result, the final database contains 15,577 records corresponding to approximately 4 hours and 20 minutes of GPS data.

4. RESULTS

Figure 6 shows a comparison between the estimated driving path curvatures with the as-built obtained from cadastral information. Figure 6 supports the conclusions of several authors (Stewart 1977, Godthelp 1986, Bonneson 2000), since drivers tend to anticipate the action on the steering wheel before the point of curvature.

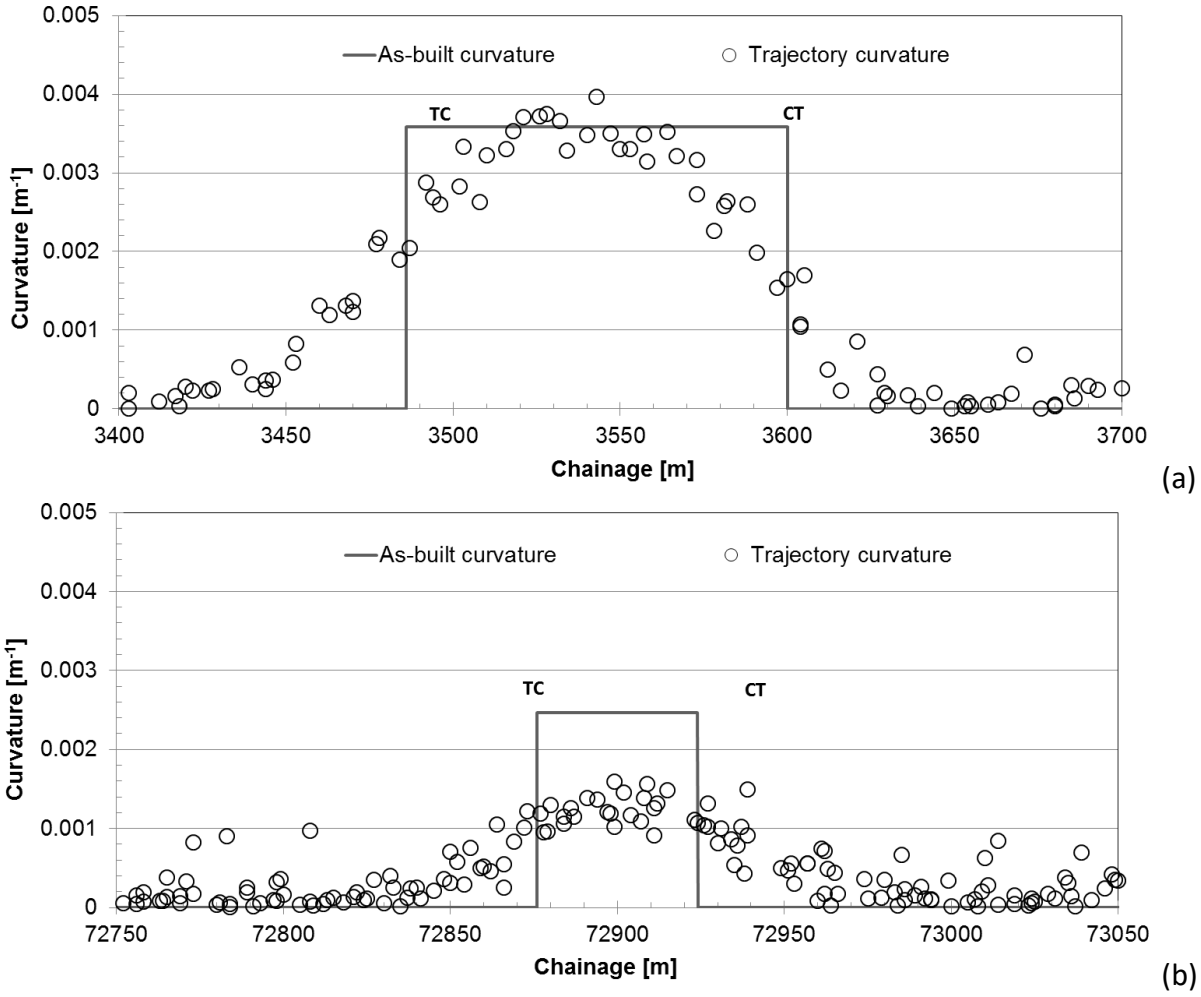

Figure 6. Comparison between as-built and vehicle trajectory curvatures for (a) R = 279.11 m, L = 113.95 m, and (b) R = 404.88 m, L = 47.51 m extracted from the database

Figure 6a shows the case of a curve along the section #1 (0.00358 m^{-1} arc curvature with a length of 113.95 m, left-hand curve). All the drivers reach the arc curvature in the central part of the curve with a significant lateral shift that lasts around 50 to 100 m across the TC and CT points. Figure 6b highlights the distance between the two curvatures along a segment of section #3 (0.00247 m^{-1} arc curvature with a length of 47.51 m, right-hand curve). The curve presents a larger radius (smaller curvature) and shorter length than the one in Figure 6a, which correspond to a lateral shift in their trajectory and the failure to reach the designed curvature. Similar results were observed in the remaining cases. It should be noted that the chainage value used to represent the curvature data corresponds to that adopted in Figure 3.

To investigate the effects of radius and length of curves on driving path, and to take into account the general behaviour of drivers who attempt to negotiate the curve by adopting a path with the least curvature, the curvature difference ($\Delta c_{i,k}$) at the i-th point located along the k-th curve was estimated. According to eq. 4, it was assumed equal to the difference between the as-built curvature ($c_{ABi,k}$) and the vehicle trajectory curvature ($c_{Ti,k}$):

$$\Delta c_{i,k} = c_{ABi,k}(s_{i,k}) - c_{Ti,k}(s_{i,k}) \quad (4)$$

where $s_{i,k}$ represents the curvilinear abscissa of the i-th point of the k-th curve.

The average curvature difference Δc_k was calculated following the trapezium approximation rule applied to non-uniform spacing ($\Delta s_{i,k}$) as per the following equation:

$$\Delta c_k = \frac{1}{s_{CT,k} - s_{TC,k}} \sum_{i=1}^{n} \left[c_{AB,k}(s_{i,k}) - c_T(s_{i,k}) \right] \cdot \Delta s_{i,k} \quad (5)$$

where $s_{CT,k}$ is the abscissa of the curve to tangent point, $s_{TC,k}$ is the abscissa of the tangent to curve point, n is the number of curvature data available along the k-th curve. Since Δc_k depends on the magnitude of curvature, the *dimensionless average curvature difference* ($\Delta c_{dl,k}$) is proposed by the following formula:

$$\Delta c_{dl,k} = \frac{\Delta c_k}{c_{AB,k}} = \Delta c_k \cdot R_{AB,k} \quad (6)$$

where $R_{AB,k}$ is the as-built radius of the k-th curve. Figure 7 provides details on the variables and parameters previously described.

$\Delta c_{dl,k}$ tends to zero when the driver follows the road alignment. Hence, it represents a measure of the capacity of the alignment to enforce appropriate driver behaviour. $\Delta c_{dl,k}$ was estimated along the 250 monitored curves, which represent a sample of the 286 investigated curves obtained with the exclusion of very short curves and curves affected by an insufficient number of data points (i.e., curves of very short length where the number of data available were too low and valid for only a few drivers).

Figure 8 reports the $\Delta c_{dl,k}$ values as a function of the curve length, with data separated into four intervals with as-built radii lower than 100 m, between 100 and 200 m, 200 and 400 m, and greater than 400 m. Results show that the dimensionless average curvature difference tends to be distributed in wider ranges when the curve length is short. When the curve length increases, the $\Delta c_{dl,k}$ range reduces progressively. The trend supports the observation of Spacek (2005): in the case of short curves, drivers exhibit different track behaviours ranging from those that tend to shift laterally adopting a wider path radius, to those that tend to follow the roadway curve. Conversely, wider and longer curves tend to be driven at the same curvature as that of the horizontal alignment.

Similarly to Figure 8, Figure 9 shows the distribution of $\Delta c_{dl,k}$ data as a function of the deviation angle of the curve. Once again, to highlight the effects of the as-built radius, data have been split into four radius ranges with different symbols. Referring to the whole data, when the deviation angle increases, $\Delta c_{dl,k}$ decreases as a function of the radius range.

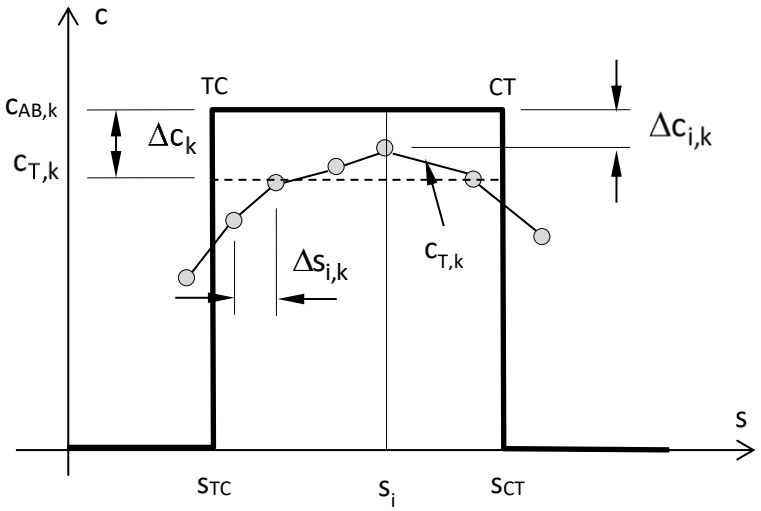

Figure 7. Diagram for the estimation of the average curvature difference (Δc_k) along the generic k-th curve from as-built ($c_{AB,k}$) and surveyed trajectory curvature ($c_{T,k}$)

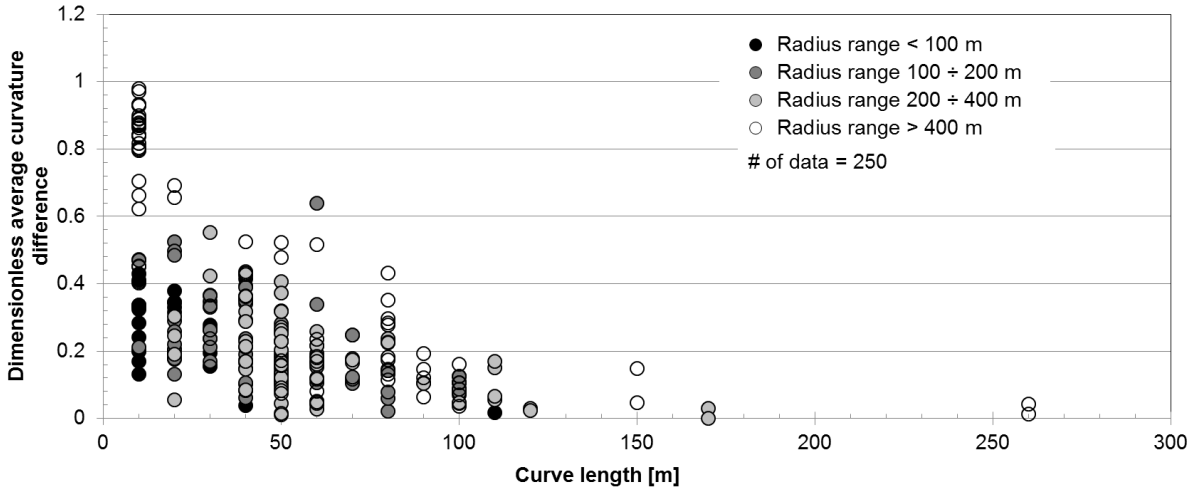

Figure 8. Relationship between the dimensionless average curvature difference and curve length

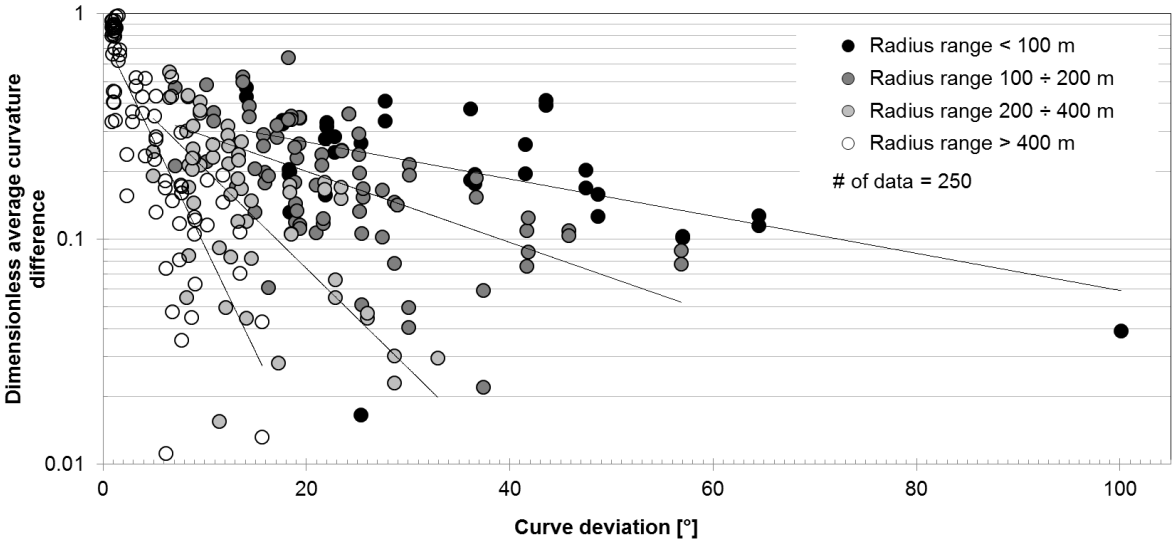

Figure 9. Relationship between the dimensionless average curvature difference and curve angle

Finally, referring to the tendency lines (exponential functions) plotted for each radius range, their intercept and slope increase passing from the radius range lower than 100 m to the range higher than 400 m.

It is worth noting that most of the radius values greater than 400 m are associated with very small deviation angles. This is attributable to the fact that designers tend to select the highest possible radius value to fillet vertex polylines with a short deviation angle to increase the travel time along the curve, thereby aiding driver perception and steering action.

5. DATA ANALYSIS AND DISCUSSION

5.1 Dimensionless average curvature difference

Starting from comments to Figure 9, data was used to calibrate a model able to link the as-built curve radius (R, in m) and the central angle (α, in sexagesimal degrees) to the dimensionless average curvature difference ($\Delta c_{dl,k}$), as per the following exponential equation:

$$\Delta c_{dl,k} = (a \cdot R + b) \cdot e^{\alpha \cdot (c \cdot R + d)} \quad (7)$$

in which the four parameters a, b, c, and d were calibrated using the least squares method, with values listed in Table 4. In the table, the four parameters have been distinguished for each sub database (Section #1, Section #2, and Section #3), as well as for the complete database (Section #1-3). It is worth noting that the calibration parameter values obtained from each sub database are very close to the values obtained using the complete database. In the case of Section #3, the number of observations (51) with respect to the number of parameters (4) is too low: hence, the parameters calibrated from the whole database should be regarded as more reliable.

Table 4 also includes three performance measurements, which support the relative forecasting accuracy between the observed and the estimated dimensionless average curvature difference, which depends on the scale of measurement. The three measurements are the *mean prediction bias* (MPB) which indicates the difference in sign between measurement (*m*) and prediction (*p*) divided by the number of data, the *mean of absolute deviations* (MAD) which averages the sum of the absolute differences between *m* and *p* divided by the number of data, and finally the *mean squared error* (MSE) that represents the squared root of the sum of squared differences between *m* and *p* divided by the number of data minus the number of parameters in the model (in this specific case equal to 4). The coefficient of determination is also reported in Table 4.

The three performance measurements and the coefficient of determination highlight the fact that the model worked well with similar coefficients in the three sections. When calibrated with the entire database, the model parameters are consistent with those derived from each sub-database. The coefficient of determination suggests that the variables included in the model are able to explain 72% of the variance in the data.

According to Bonneson (2000), curves of short length (i.e., small angles of deviation) are prone to be driven with trajectories of lower curvature, while longer curves are driven with curvatures almost equal to the alignment curvature. Figure 10a shows the effects of the combination of deviation angle (α) and radius of a curve (R), exploring the field of validity of eq. 7 (25.59 m ≤ R ≤ 1369.98 m, 0.84° ≤ α ≤ 100.09°). In the figure, the higher $\Delta c_{dl,k}$ the lower the conditioning effect of the curve on driven trajectories. Figure 10a also explains the combination of radius and deviation angle that can be associated with values of $\Delta c_{dl,k}$ that tend to zero. Figure 10b shows a comparison between the as-built curve radii and the average trajectory radii estimated according to the following formula:

$$R_k = \frac{1}{\overline{c_{T,k}}} \quad (8)$$

where $\overline{c_{T,k}}$ is the average curvature estimated with:

$$\overline{c_{T,k}} = \frac{\sum_{i=1}^{n} c_{Ti,k}}{i} \quad (9)$$

Figure 10b demonstrates that R_k is always greater than the as-built radius, thus confirming that drivers tend to use a larger radius than the design one. Moreover, when the as-built curve radius increases, the difference between it and the trajectory curve increases too. In these cases, the more dispersed data are associated with smaller deviation angles, where drivers tend to use larger radii than those of the road alignment, thus confirming the inferences drawn from Figure 10a.

Table 4. Synthesis of model coefficients for eq. 7, and performance measurements results

Model coefficients	**Section #1**	**Section #2**	**Section #3**	**Sections #1-3**
a	0.05	0.08	0.04	0.06
b	40.88	34.58	50.09	43.71
c	-0.0003	-0.0003	-0.0002	-0.0003
d	0.002	0.007	-0.013	-0.003
Statistics				
# of data	112	87	51	250
Mean prediction bias, MPB	-0.10	0.38	0.004	0.08
Mean of absolute deviations, MAD	10.00	7.87	7.30	8.71
Mean squared error, MSE	188.71	115.7	91.30	139.3
Coefficient of determination (R^2)	0.72	0.77	0.67	0.72

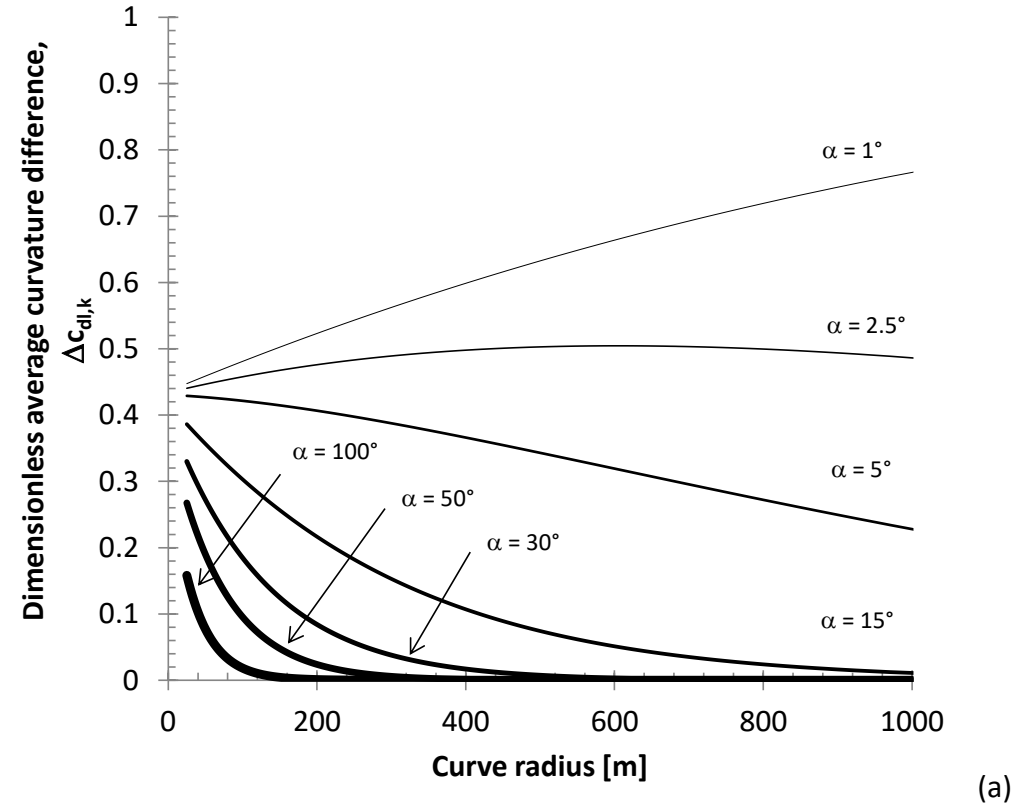

(a)

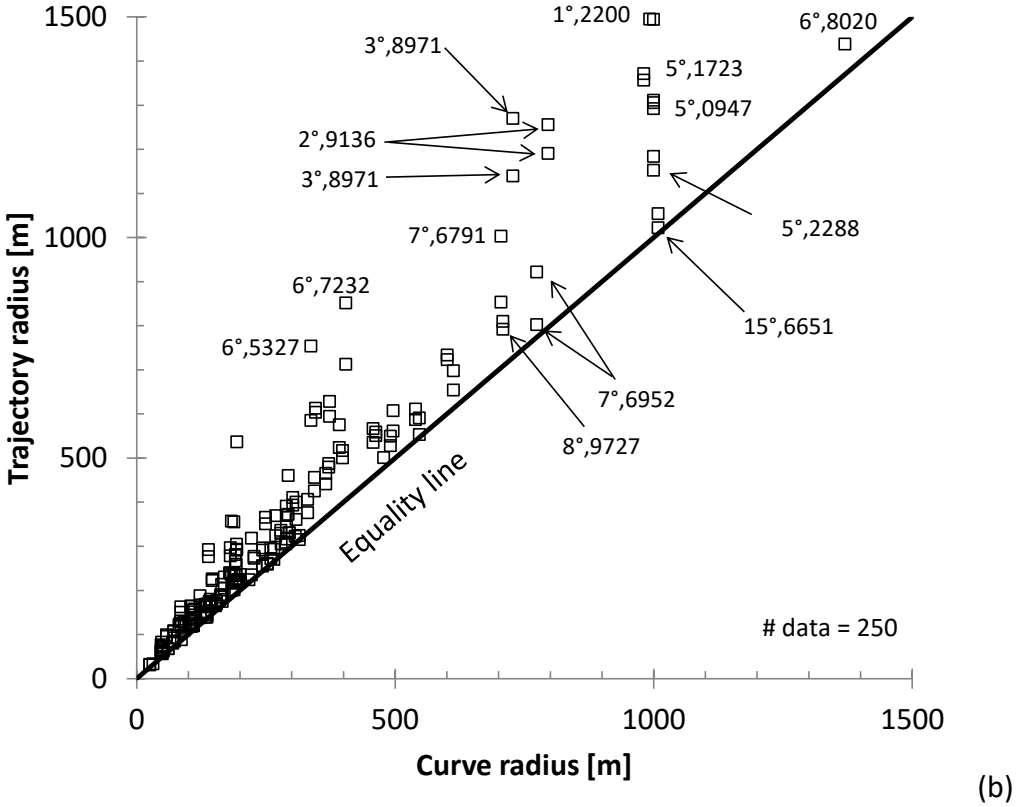

(b)

Figure 10. (a) Sensitivity analysis of eq. 10, and (b) relationship between average curve radius and trajectory radius

5.2 Curvature of driving path

The spatial data points collected in the investigation have also been used to calibrate a model that can be used to predict the trajectory curvature (c_T). Considerations included in Paragraph 3 suggest that drivers anticipate the steering action when negotiating a curve. Although this action results primarily from a visual interpretation of the geometrics of the road environment ahead of and surrounding the driver, it is also influenced by the geometry of the elements just traversed.

On the basis of these considerations, a discrete model structure reflecting general driver behaviour as affected by the road characteristics in terms of trajectory selected is proposed here. The model was structured as a moving average with weighted factors that decrease as the distance from the point under consideration increases. The curvature at a generic point i of vehicle trajectories ($c_{T,i}$) is supposed to be dependent on the as-built horizontal alignment curvature, with curvature values defined for a certain pace along the road chainage. The equation model is as follows:

$$c_{T,i} = \frac{\sum_{h=i-n}^{h=i+n} c_{AB,h} \cdot p_h}{\sum_{h=i-n}^{h=i+n} p_h} \qquad (10)$$

where, $c_{AB,h}$ indicates the as-built horizontal alignment at a generic point h located in a range across the i-th point, p_h represents a weighted factor variable as a function of the distance from the generic h-th point, n indicates the number of points preceding and following the i-th assumed to estimate step by step the trajectory curvature c_T.

The model envisages the discretization of the as-built horizontal alignment into a sequence of spatial points. Eq. 10 evidences that c_T is estimated as a linear combination of c_{AB} values close to the i-th point. These points are associated with the weighted factors that decrease progressively from the reference value 100 for the i-th point (p_i = 100), to the i-n (preceding) and i+n (following) points, according to:

$$p_{i+j} = \frac{p_{i+(j-1)}}{Y'} \qquad (11)$$

$$p_{i-j} = \frac{p_{i-(j+1)}}{Y''} \qquad (12)$$

where j varies between 1 and n.

It is worth noting that the set of model equations (i.e., eq. 10, 11 and 12) includes the two calibration factors, Y' and Y". These modulate the memory effect of the horizontal alignment already driven (Y"), and the observed horizontal alignment that has to be driven (Y'). To calibrate them, an interval of 10 m between points and the least squares method were adopted.

The values of model parameters and the dispersion measurements already used in Table 4 are reported in Table 5, distinguishing once again the calibration of each road section from that carried out on the entire database made up of 15,577 data. The differences between model parameters and performance measurements are not significant and the values observed for the full investigated length are in the ranges of the three investigated sections. Finally, the coefficients of determination are relatively high, confirming that the model can accurately predict the curvature of real trajectories.

The values of the Y parameters are quite different for the three sections. This reflects the differences in the curvature values presented in Figure 3, where the curvature distribution and magnitude of Section #1 and #2 are similar, while Section #3 presents some curves with greater curvatures (i.e., small curve radii). It is worth noting that the greater Y is, the shorter is the road section affecting the driven curvature.

Figure 11 proposes a comparison between the as-built horizontal alignment curvature (c_{AB}), the observed curvature data of all the vehicles and drivers involved in the investigation and the modelled curvatures obtained according to eq. 10, with the model parameters calibrated on the entire database (Y' = 2.343, Y" = 2.162). In the figure, all the data are reported in absolute values. Referring to Figure 3, the three graphs of Figure 10 provide a comparison of a 2 km stretch of Sections #1, #2 and #3 respectively, for direction A.

Table 5. Synthesis of calibration factors for eq.11 and 12, and performance measurements results

Calibration factors	**Section #1**	**Section #2**	**Section #3**	**Sections #1-3**
Y'	1.81	1.84	2.29	2.343
Y"	1.84	1.95	2.55	2.162
Statistics				
# of data	5,354	4,822	5,401	15,577
Mean prediction bias, MPB	0.00012	0.00014	0.00051	0.00025
Mean of absolute deviations, MAD	0.00058	0.00035	0.00093	0.00025
Mean squared error, MSE	$1.25 \cdot 10^{-6}$	$3.15 \cdot 10^{-7}$	$3.47 \cdot 10^{-6}$	$1.78 \cdot 10^{-6}$
Coefficient of determination (R^2)	0.84	0.94	0.90	0.90

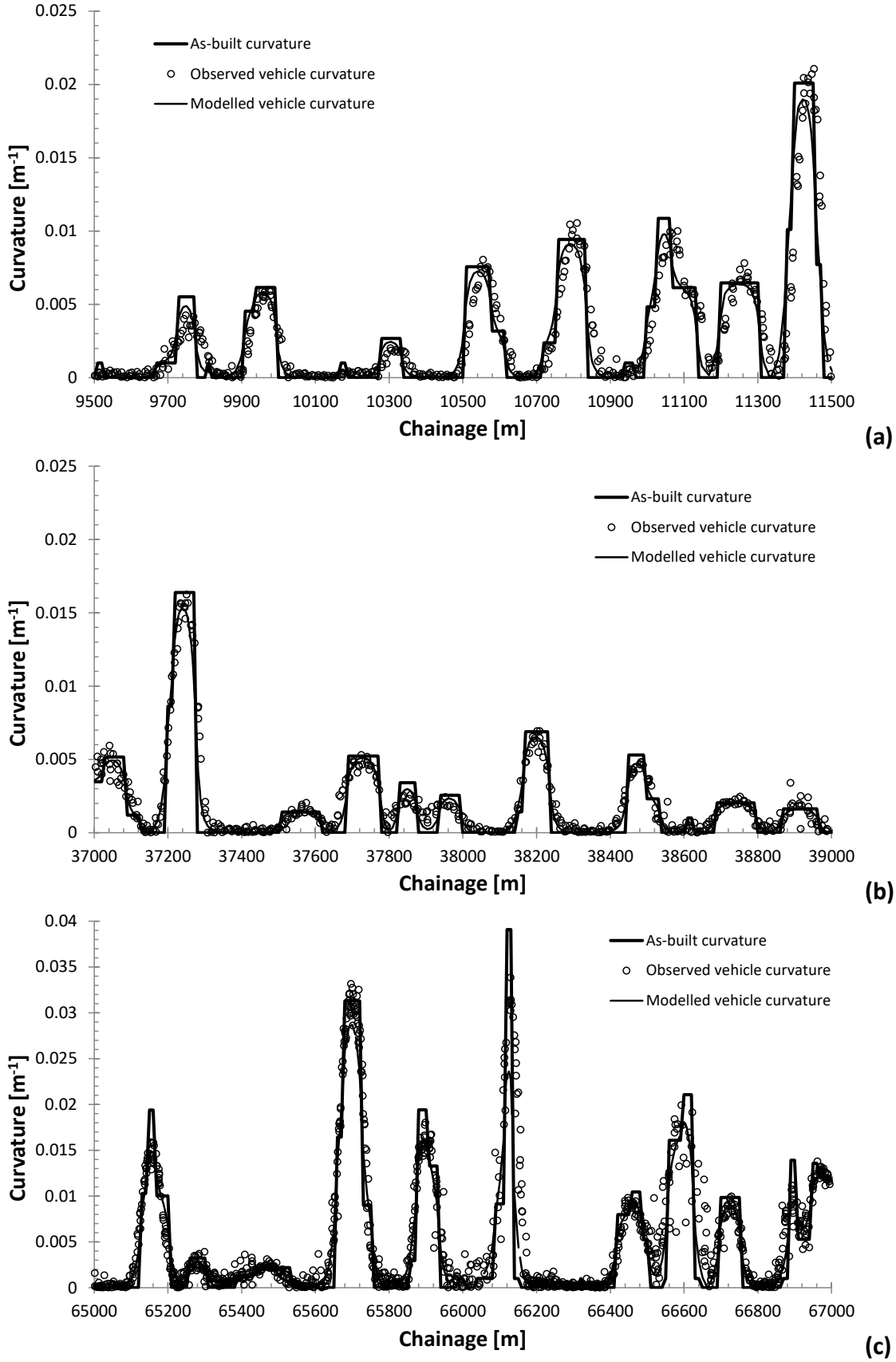

Figure 11. As-built curvature, observed and modelled trajectory vehicle curvature comparison along a portion of the three sections (direction A).

A good correlation between observations and model outputs is evident in Figure 12. Most of the data are close to the equality line that indicates the perfect model prediction. Data far from the equality line are few and mostly concentrated close to the origin, in which very small curvature data relate to points along tangents. To highlight the model quality, Table 6 contains the number of data that falls into several intervals across the equality line: it is worth noting that more than 83% of the data falls into the closest interval at ± 0.001 m^{-1}.

Figure 13 shows the evolution of the weighted p_i factors (eq. 11 and eq.12) in which the reference point is placed at the conventional chainage of 500 m. Figure 13 also contains the evolution of Y' and Y" for the speed model proposed in Cafiso and Cerni (2012), which was used in a similar manner and on the same highways to estimate percentiles of operating speeds along a road alignment.

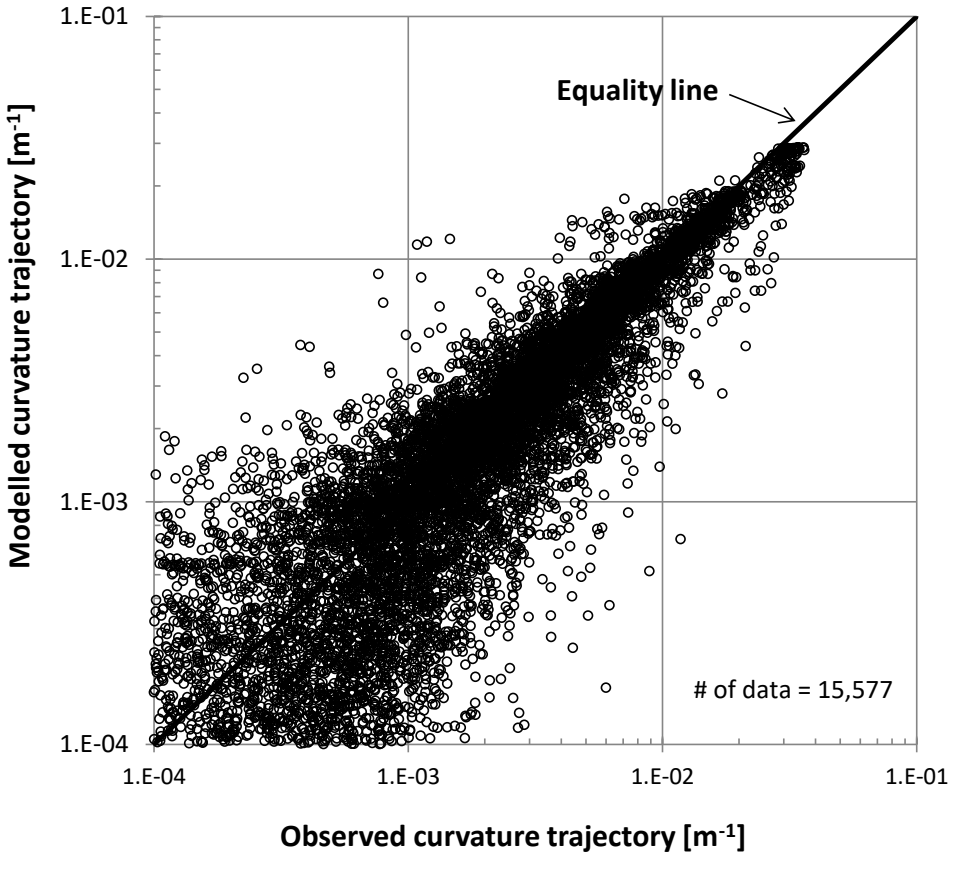

Figure 12. Comparison between the observed and modelled trajectory curvature

Table 6. Synthesis of data distribution in Figure 12 around the equality line

Interval	±0.001	±0.002	±0.003	±0.004	±0.006	±0.008	±0.010	±0.019
# data in the interval	12,955	14,567	15,044	15,247	15,422	15,499	15,533	15,577
# data outside the interval	2,619	1,007	530	327	152	75	41	0
% of data in the interval	83.2	93.5	96.6	97.9	99.0	99.5	99.7	100.0

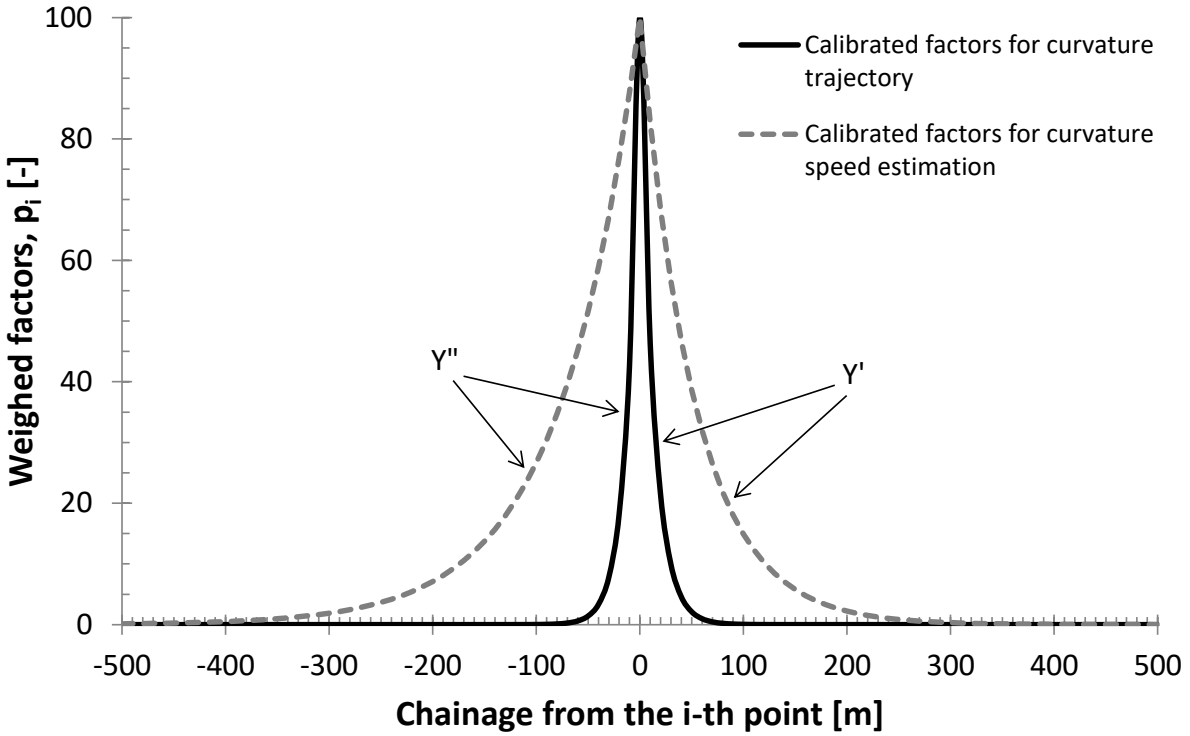

Figure 13. Distribution of p_i values as a function of calibration factors for curvature trajectory and for operating speed estimation according to Cafiso and Cerni (2012).

From a comparison of the two curves, it is evident that the p_i values for trajectory estimation decrease more rapidly around the i-th point than the equivalent calibration factors for operating speeds. The most significant p_i values that control the evolution of $c_{T,i}$, for example those that are greater than 0.01, fall into the range of -55 ÷ 60 m around the i-th point. Conversely, in the case of operating speeds the corresponding significant p_i values fall into the range -345 ÷ 245 m around the i-th point.

This result supports the inference that drivers are prone to selecting driving curvatures on the basis of (their) recent driving experience and from observation of a very small road section across each position. Vice versa, the driver adopts operating speeds on the basis of longer sections along the same road. In other words, speed and track behaviours are affected by different lengths of the same road section.

6. CONCLUSIONS

In this paper, the authors present two driver-behaviour models calibrated along sections of two-lane rural highways. These were investigated by carrying out naturalistic surveys with vehicles equipped with high accuracy GPS in RTK mode. Positioning data were collected for the creation of a robust database composed of 15,577 positioning data that were used to estimate trajectory curvatures.

A first model concerns the estimation of the "dimensionless average curvature difference" ($\Delta c_{dl,k}$), which measures the difference between the curvature of the horizontal alignment and the curvature of trajectories. $\Delta c_{dl,k}$, with values observed in a range between 0 and 1 and which can be used to explain the tendency of drivers to adopt different trajectory curvatures (normally lower) to those assumed by designers. The model highlights how drivers tend to follow the designed alignment only for specific combinations of deviation angle and curve radius. At present, the authors are not able to provide an acceptable limit for $\Delta c_{dl,k}$ useful for providing information on possible geometric adjustments, since this has to be assessed on the basis of agreed safety limits.

A second model regards the estimation of the trajectory curvature (c_T) which is expressed as a function of the as-built horizontal alignment curvature (c_{AB}). Together with the operating speed model developed in Cafiso and Cerni (2012), the trajectory driving model proposed here should be of assistance to the designer when seeking to predict the effects of road alignment on driver behaviour. The two models are simple to use and can be recalibrated on tracking data collected from different road geometrics, road typologies, and road environments.

Future aims include a validation of the models with new curvature data from new highway sections in order to increase their statistical relevance. An extension of their range of application is also envisaged with data collected from different road categories. Furthermore, the authors will use the second model to investigate the relationship between operating speed and trajectory curvature and establish any links between this relationship and the high crash frequency of certain combinations of road design elements (tangents, curve, transition curves).

ACKNOWLEDGEMENTS

The authors would like to thank the Province of Perugia (Italy), in particular the staff of the Traffic Management Department, for their support during the GPS field surveys. The help of Giulia Brugnami with the organization of the database was greatly appreciated.

REFERENCES

AASHTO (American Association of State Transportation Officials, 2010). *Highway Safety Manual*. AASHTO, Washington, D.C.

Bonneson, J. (2000). Kinematic approach to horizontal curve transition design. *Transportation Research Record*, 1737, 1-8.

Cafiso, S., Cerni, G. (2012). New approach to defining continuous speed profile models for two-lane rural roads. *Transportation Research Record*, 2309, 157-167.

Coifman, B., Beymer, D., McLauchlan, P., Malik, J. (1998). A real-time computer vision system for vehicle tracking and traffic surveillance. *Transportation Research Part C: Emerging Technologies*, 6(4), 271-288.

Coutton-Jean, C., Mestre, D. R., Goulon, C., Bootsma, R. J. (2009). The role of edge lines in curve driving. *Transportation Research Part F: Traffic Psychology and Behaviour*, 12(6), 483-493.

Dijksterhuis, C., Brookhuis, K. A., De Waard, D. (2011). Effects of steering demand on lane keeping behaviour, self-reports, and physiology. A simulator study. *Accident Analysis & Prevention*, 43(3), 1074-1081.

Donnell, E., Himes, S., Mahoney, K., Porter, R. (2009). Understanding speed concepts: key definitions and case study examples. *Transportation Research Record*, 2120, 3-11.

Fitzpatrick, K., Wooldridge, M.D., Tsimhoni, O., Collins, J.M., Green, P., Bauer, K.M., Parma, K.D., Koppa, R., Harwood, D.W., Anderson, I., Krammes, R.A., Poggioli, B. (2000). *Alternative design consistency rating methods for two-lane rural highways*. Federal Highway Administration, FHWA-RD-99-172.

Fitzsimmons, E.J., Nambisan, S.S., Souleyrette, R.R., Kvam, V. (2013). Analyses of Vehicle Trajectories and Speed Profiles Along Horizontal Curves. *Journal of Transportation Safety & Security*, 5(3), 187-207.

Friedinger, C. (1980). Information and driver behavior while passing through curves. Thesis dissertation, ETH, Zurich.

Glennon, J. C., Harwood, D. W. (1978). Highway design consistency and systematic design related to highway safety. *Transportation Research Record*, 681, 77-88.

Godthelp, H. (1986). Vehicle control during curve driving. *Human Factors: The Journal of the Human Factors and Ergonomics Society*, 28(2), 211-221.

Hancock, P.A., Wulf, G., Thom, D., Fassnacht, P. (1990). Driver workload during differing driving maneuvers. *Accident Analysis & Prevention*, 22(3), 281-290.

Hills, B. L. (1980). Vision, visibility, and perception in driving. Perception, 9(2), 183-216.

Horberry, T., Anderson, J., Regan, M. A. (2006). The possible safety benefits of enhanced road markings: a driving simulator evaluation. *Transportation Research Part F: Traffic Psychology and Behaviour*, 9(1), 77-87.

Lamm, R., Psarianos, B., Mailaender, T. (1999). *Highway design and traffic safety engineering handbook*. McGraw-Hill Handbooks.

Lamm, R., Choueiri, E. M., Psarianos, B., Soilemezoglou, G. (1995, August). A Practical Safety Approach to Highway Geometric Design. International Case Studies: Germany, Greece, Lebanon, and the United States. In *1st International Symposium on Highway Geometric Design*, Boston, Massachusetts

Land, M.F., Lee, D.N. (1994). Where we look when we steer. *Nature*, 369 (6483), 742-744.

Land, M., Horwood, J. (1995). Which parts of the road guide steering? *Nature*, 377(6547), 339-340.

McKnight, A. S., McKnight, A. J., Tippetts, A. S. (1998). The effect of lane line width and contrast upon lanekeeping. *Accident Analysis & Prevention*, 30(5), 617-624.

Messelodi, S., Modena, C. M., Zanin, M. (2005). A computer vision system for the detection and classification of vehicles at urban road intersections. *Pattern Analysis and Applications*, 8(1-2), 17-31.

Messer, C.J. (1980). Methodology for Evaluating Geometric Design Consistency. *Transportation Research Record*, 757, 7-14.

Mussone, L., Matteucci, M., Bassani, M., Rizzi, D. (2013). An innovative method for the analysis of vehicle movements in roundabouts based on image processing. *Journal of Advanced Transportation*, 47(6), 581-594.

Patire, A.D., Wright, M., Prodhomme, B., Bayen, A.M. (2015). How much GPS data do we need? *Transportation Research Part C*, 58, 325–342

Post, T. J., Alexander, G. J., Lunenfeld, H. (1981). *A User's Guide to Positive Guidance* (No. FHWA-TO-81-1).

Prokop, G. (2001). Modeling human vehicle driving by model predictive online optimization. *Vehicle System Dynamics*, 35(1), 19-53.

Repubblica Italiana (2001a). Norme funzionali e geometriche per la costruzione delle strade. Decreto Ministeriale 5 Novembre 2001, No. 6792 (in Italian).

Repubblica Italiana (2001b). Modalità di istituzione e aggiornamento del catasto delle strade ai sensi dell'art. 13, comma 6, del decreto legislativo 30 Aprile 1992, n. 285, e successive modificazioni. Decreto Ministeriale 1 giugno 2001, No. 3483 (in Italian).

Schnell, T., Zwahlen, H. (1999). Driver preview distances at night based on driver eye scanning recordings as a function of pavement marking retroreflectivities. *Transportation Research Record: Journal of the Transportation Research Board*, 1692, 129-141.

Stewart, D (1977). The Case of the Left-Hand Bend. *The Highway Engineer*, 24(6), 12–17.

Spacek, P. (2005). Track behavior in curve areas: attempt at typology. *Journal of Transportation Engineering*, 131(9), 669-676.

Tang, J., Song, Y., Miller, H.J., Zhou, X. (2016). Estimating the most likely space–time paths, dwell times and path uncertainties from vehicle trajectory data: A time geographic method. *Transportation Research Part C*, 66, 176–194

Transportation Research Circular (2011). *Modeling operating speed*. E-C151 Synthesis Report, Transportation Research Board of the National Academies, Washington, DC.

Williams, T., Alves, P., Lachapelle, G., Basnayake, C. (2012). Evaluation of GPS-based methods of relative positioning for automotive safety applications. *Transportation Research Part C*, 23, 98–108